FULL TITLE PAGE

Manuscript Title

Intra-Procedural C-Arm Dual-Phase Cone-Beam CT Imaging to Predict Response of Hepatocellular Carcinoma During Drug-Eluting Beads Transcatheter Arterial Chemoembolization

Manuscript Type

Original Research

Authors and Affiliations

Romaric Loffroy, MD [(1)], MingDe Lin, PhD [(2)], Gayane Yenokyan, PhD [(3)], Pramod P. Rao, MD [(1)], Nikhil Bhagat, MD [(1)], Niels Noordhoek, PhD [(4)], Alessandro Radaelli, PhD [(4)], Järl Blijd, MSc [(4)], Eleni Liapi, MD [(1)], Jean-François Geschwind, MD [(1)]

[(1)] Russell H. Morgan Department of Radiology and Radiological Science, Division of Vascular and Interventional Radiology, Johns Hopkins Hospital, Baltimore, MD, USA

[(2)] Clinical Informatics, Interventional, and Translational Solutions (CIITS), Philips Research North America, Briarcliff Manor, NY, USA

[(3)] Johns Hopkins Biostatistics Center, Johns Hopkins Bloomberg School of Public Health, Baltimore, MD, USA

[(4)] Philips Healthcare, Best, The Netherlands

Corresponding Author

Jean-François Geschwind, MD

Professor of Radiology, Surgery and Oncology

Section Chief, Cardiovascular and Interventional Radiology

Director, Interventional Radiology Research Center

Professional address: The Russell H. Morgan Department of Radiology and Radiological Science, Division of Vascular and Interventional Radiology, The Johns Hopkins Hospital, 600 North Wolfe Street, Blalock 545, Baltimore, MD 21287, USA

Tel: (001)-410-955-6081

Fax: (001)-410-955-0233

E-mail: jfg@jhmi.edu

Funding and Financial Support

This study was funded by the French Society of Radiology and supported by a Grant from Philips Research North America, Briarcliff Manor, NY, USA

Statement

This paper has not been presented at any RSNA meeting and has not been accepted for presentation at any future meeting

Word Count

Introduction to Discussion: 3943

ABBREVIATED TITLE PAGE

Manuscript Title

Intra-Procedural C-Arm Dual-Phase Cone-Beam CT Imaging to Predict Response of Hepatocellular Carcinoma During Drug-Eluting Beads Transcatheter Arterial Chemoembolization

Manuscript Type

Original Research

Advance in Knowledge

Dual-phase cone-beam CT (DPCBCT) technology allows for hepatocellular carcinoma (HCC) imaging at both early and delayed arterial phases using only one contrast injection during drug-elutings bead transarterial chemoembolization (DEB-TACE)

A statistically significant relationship exists between post-DEB-TACE DPCBCT HCC enhancement and objective MRI HCC 1-month response, indicating that DPCBCT may be used during DEB-TACE to predict HCC 1-month response

Implications for Patient Care

DPCBCT technique should be included into the very early intra-procedural assessment of therapy response in patients with HCC who undergo DEB-TACE

Summary Statement

This study demonstrates that intra-procedural DPCBCT imaging can be used at the time of DEB-TACE to predict HCC 1-month MRI response

ABSTRACT

Purpose: To investigate whether intra-procedural dual-phase C-arm cone-beam CT (DPCBCT) can predict hepatocellular carcinoma (HCC) 1-month response during drug-eluting beads transcatheter arterial chemoembolization (DEB-TACE).

Materials and Methods: IRB approval and patient informed consent were obtained for this prospective HIPAA-compliant study. Forty-seven targeted lesions in 27 patients (15 male; 12 female; mean age, 61.9±10.7 years) with unresectable HCC treated using DEB-TACE on a DPCBCT capable C-arm interventional radiology system were analyzed. MRI was performed 1 month before and after DEB-TACE. Intra-procedural DPCBCT imaging was done prior to and immediately following DEB-TACE. Pre- and post-procedural CBCT tumor enhancement (TE) at early- and delayed arterial-phases was assessed blind to MRI findings. Tumor response (TR) was measured according to European Association for the Study of the Liver (EASL) criteria. Logistic regression models for the correlated data were used to assess and compare changes in TE between modalities.

Results: An objective (complete or partial) EASL TR was achieved in 74.5% and 76.6% of lesions at 1 month post-DEB-TACE on MR arterial- and portal venous-phases, respectively. Paired T-tests comparing pre- and post-DEB-TACE TE showed statistically significant average reduction in TE for both modalities by phase and lesion (P<0.0001). CBCT TE decrease post-DEB-TACE linearly correlated with MRI, estimated correlation coefficient was excellent for both first (0.79) and second (0.67) phases. A statistically significant relationship between post-DEB-TACE CBCT TE and objective MRI TR was found for both first (OR, 0.95; 95%CI, 0.91-0.99;

P=0.023) and second (OR, 0.96; 95%CI, 0.93-0.99; *P*=0.035) phases, respectively, in the multivariate logistic regression model.

Conclusion: Intra-procedural DPCBCT technology can be used at the time of DEB-TACE to predict 1-month EASL HCC response.

KEYWORDS

Hepatocellular carcinoma; Transcatheter arterial chemoembolization; Drug-eluting beads; C-arm cone-beam CT; Magnetic resonance imaging.

INTRODUCTION

Hepatocellular carcinoma (HCC) is the third most common cause of cancer death worldwide (1). The majority of patients present with intermediate or advanced disease that is not amenable to curative treatment, and the median survival in this group is 6 to 8 months (2). Well-designed randomized trials have shown the positive impact of transcatheter arterial chemoembolization (TACE) on increasing the survival for these patients (3,4). The conventional chemoembolizing agent used is a lipiodol-chemotherapy suspension. While there has been success, this 30+ year old anti-cancer cocktail has significant side-effects, including pain, low level fevers, and nausea and vomiting (post-embolization syndrome) that diminishes the quality of life after the procedure. As such, a new type of chemoembolizing agent has been developed in the recent years using microspheres with drug-eluting capabilities that can be administered intra-arterially in the same manner as conventional TACE. These microspheres or drug-eluting beads (DEBs) allow for controlled and sustained drug delivery and minor blood dispersion of the drug compared with conventional TACE (5,6). The first clinical studies with TACE using DEBs (DEB-TACE) in the treatment of HCC showed a high index of tumor necrosis, a low incidence of toxicities, and overall response rates varying from 50% to 75%, even for patients with advanced HCC (7–11).

Early assessment of the effectiveness of TACE and monitoring tumor response are paramount to identify treatment failure, to help guide future therapy, and to determine the time interval of repeat treatment. Conventionally, response is evaluated by magnetic resonance imaging (MRI) at 1-3 months after TACE according to the Response Evaluation Criteria in Solid Tumors (RECIST) (12–14). However,

assessment of anatomical response in the early post-treatment period can be misleading because a reduction in tumor size often does not correlate with the degree of tumor necrosis (15,16). Consequently, reduction of tumor enhancement as seen on imaging has been used more accurately as a biomarker of tumor response, as proposed by the European Association for the Study of Liver Disease (EASL) (15,17). Post-TACE treatment response is evaluated by MRI 1-3 months after treatment, too late for intra-procedural treatment modification. Furthermore, the time frame is not standardized, and can be too long of a wait for patients who need sooner retreatment. So an imaging modality that can serve as an early surrogate marker of tumor necrosis, and objectively predict future tumor response at the time of treatment, would be immensely beneficial, especially because treatment response has been identified as an independent predictor of survival (3). It has been recently reported that intra-procedural apparent diffusion coefficient (ADC) changes assessed in a hybrid magnetic resonance/interventional radiology (MR/IR) suite can predict 1-month anatomical HCC response and provide valuable feedback at the time of TACE (18). However, main drawbacks are the poor worldwide availability of hybrid MR/IR suites and the need for multiple patient transfers between the x-ray unit and the adjacent MR unit during the TACE procedure. Recently, C-arm computed tomography (CT) has emerged as a new and more popular generation of imaging technology available in the angiography suite, allowing for the acquisition of a three-dimensional dataset generated from one rotational run with the use of cone-beam CT principles (CBCT) (19-23). Early clinical experience has demonstrated C-arm CT imaging to be a useful adjunct to digital subtraction angiography (DSA) for use in hepatic vascular intervention procedures (19,22). It can be used notably to visualize tumor feeding vessels and parenchymal staining during TACE. All current

commercially available CBCT systems necessitate two separate contrast-enhanced scans. A recent development is the ability to capture these two phases using only one contrast agent injection, C-arm dual-phase CBCT (DPCBCT) (26,27). To our knowledge, no study has shown whether DPCBCT technology could be used during TACE to predict future tumor response.

Therefore, we tested the hypotheses that percent change in tumor enhancement can be assessed at the time of DEB-TACE using intra-procedural C-arm dual-phase CBCT technology, and that this percentage can predict conventional MR anatomical image changes at 1-month post-DEB-TACE. More specifically, our objective was to prospectively investigate whether intra-procedural C-arm DPCBCT imaging can predict EASL response of unresectable HCC at 1-month post-DEB-TACE.

MATERIALS AND METHODS

Study Cohort

This single-institution prospective study was compliant with the Health Insurance Portability and Accountability Act, and was approved by our Institutional Review Board. All patients provided written informed consent before inclusion in the study. The study was open for enrollment from March 2, 2009, to April 5, 2010. During this period, our liver tumor board discussed the care of 47 patients with HCC who underwent one or more cycles of DEB-TACE. Eligibility criteria for performing DEB-TACE included a confirmed diagnosis of unresectable HCC by biopsy or typical radiological findings, in addition to an elevated serum alpha-fetoprotein (> 400 ng/mL), Eastern Cooperative Oncology Group (ECOG) performance status ≤ 2, Child-Pugh classification A, B or C, focal or multifocal hepatic malignancy, absent or traces ascites, albumin > 2.5 g/dL, alanine aminotransferase and aspartate aminotransferase < 5 x upper normal limit, total serum bilirubin < 3.0 mg/dL, serum creatinine < 2.0 mg/dL, platelet count ≥ 50,000/mm^3, international normalized ratio (INR) ≤ 1.5, a left ventricle ejection fraction of ≥ 50%, absence of complete occlusion of the portal venous system, and no contraindications to MRI. Our study group included all patients with HCC who were undergoing DEB-TACE for the first time and who had undergone dynamic contrast-enhanced MR imaging before and 1 month after DEB-TACE, and intra-procedural DPCBCT pre- and post-DEB-TACE. Of the 47 patients who underwent treatment, 27 fulfilled these inclusion criteria. Patients with well-defined and infiltrative tumors were included in the study. However, patients with small tumors (< 1 cm in diameter) (n = 2) were excluded from our study because enhancement of these tumors was difficult to assess. Patients who had

undergone TACE previously (*n* = 16) were also excluded because they may have partially responded to initial therapy. Lastly, patients with poor DPCBCT image quality (*n* = 2) because of severe image artifacts were also excluded.

DEB-TACE Protocol

All DEB-TACE procedures were performed by two experienced interventional radiologists (J.F.G., N.B.; 13 and 5 years of experience, respectively) using a consistent approach. LC Beads (2 mL, BioCompatibles Ltd., Surrey, UK) with a diameter of 100 to 300 µm or 300 to 500 µm were loaded with 100 mg of doxorubicin hydrochloride (25 mg/mL, Pharmacia-UpJohn, New Jersey, USA) and mixed with an equal volume of nonionic contrast media (Oxilan 300 mg I/mL, Guerbet LLC, Bloomington, IN). Access to the common femoral artery was obtained with the Seldinger technique, and a catheter was positioned as closely to the tumor bed as possible before infusions of the DEBs. This means that every injection was performed in a superselective manner preferably through a microcatheter. DEBs (up to 4 mL) were administered by alternating aliquot injections of the beads and contrast, until complete delivery or when the blood flow of the feeding artery slowed down substantially. Complete occlusion of the main feeding artery was avoided to allow for retreatment if necessary as it has been reported before with conventional TACE technique (24).

C-Arm Dual-Phase Cone-Beam CT Technique

All patients underwent C-arm DPCBCT scan prior to and immediately following DEB-TACE therapy. The imaging was performed using a commercially available angiographic system (Allura Xper FD20, Philips Healthcare, Best, The

Netherlands). This system was equipped with the XperCT option, enabling C-arm cone-beam CT acquisition and volumetric image reconstruction (Feldkamp back projection) (25). For each CBCT scan, the area of interest was positioned in the system isocenter, and over approximately 10 seconds, 312 projection images (30 frames per second) were acquired with the motorized C-arm covering a 200° clockwise arc at 20° per sec rotation speed. As the images were being acquired, the projections were transferred via fiber optic to the reconstruction computer to produce volumetric data.

The dual-phase CBCT prototype feature modified the XperCT option to be able to acquire of two sequential, back-to-back CBCT scans so both early and delayed arterial phases are captured using only one contrast injection [26,27]. In this study, the two scans were triggered at 3 and 28 sec following a selective single injection of undiluted contrast medium through a 3-French co-axial microcatheter placed into the vessel expected to feed the targeted tumors. The same contrast injection protocol was applied to all cases (amount, 20 mL; rate, 2 mL/sec; Oxilan 300 mg I/mL, Guerbet LLC, Bloomington, IN). The patients were instructed to be at end expiration apnea during each of the CBCT scans with free breathing between the early and delayed arterial phase scans. Oxygen was administered to patients during the procedure to minimize the discomfort of breath holding. One millimeter isotropic images were 3D reconstructed from the DPCBCT scans.

MR Imaging Technique

All patients underwent baseline and follow-up (approximately 1 month prior to and 1 month following initial DEB-TACE, respectively) MR imaging using a 1.5-T MR unit (CV/I, GE Medical Systems, Milwaukee, WI, USA) and a phased-array torso

coil. The imaging protocol included: 1) axial T2-weighted fast spin-echo images (TR/TE, 5000/100 msec; matrix size, 256 x 256; slice thickness, 8-mm; interslice gap, 2-mm; receiver bandwidth, 32-kHz), 2) axial single-shot breath-hold gradient-echo diffusion-weighted echo-planar images (TR/TE, 5000-6500/110 msec; matrix size, 128 x 128; slice thickness, 8-mm; interslice gap, 2-mm; *b* value, 500 sec/mm^2; receiver bandwidth, 64-kHz), and 3) axial breath-hold unenhanced and contrast-enhanced (0.1 mmol/kg IV of gadodiamide, Omniscan, General Electric, Princeton, NJ) T1-weighted 3D fat-suppressed spoiled gradient-echo images (TR/TE, 5.1/1.2 msec; field of view, 320-400 mm^2; matrix size, 192 x 160; slice thickness, 4-6-mm; receiver bandwidth, 64-kHz; flip angle, 15°) in the arterial and portal venous phases (20 and 60 seconds after intravenous contrast administration, respectively).

Imaging Data Evaluation

The MRI and DPCBCT images were evaluated offline and were interpreted by consensus of two experienced MR/CT radiologists (R.L., P.R.; 7 and 6 years of experience, respectively) in the same reading session to ensure careful comparison of pre-DEB-TACE and sequential post-DEB-TACE MR imaging findings. The two readers assessed anatomical tumor response on T1-weighted contrast-material-enhanced MRI. In the same way, intra-procedural DPCBCT images pre- and post-DEB-TACE were analyzed during a second reading session, 2 weeks later, blinded to the MRI findings. For each patient, the targeted tumor only was evaluated in case of unifocal HCC, and the two largest targeted tumors were evaluated in case of multifocal HCC to ensure independent sampling. A reader (R.L.) used electronic calipers to record the size of the targeted tumors (one-dimensional measure of the longest dimension in keeping with the RECIST criteria) (12–14) on the portal venous

phase MR images pre- and post-DEB-TACE. Change in tumor size was calculated according to the MR images as a % change using the following formula: [(longest dimension before DEB-TACE – longest dimension after DEB-TACE)/longest dimension before DEB-TACE] x 100%. The two readers visually assessed the percentage of tumor image enhancement for the arterial MR- and early arterial DPCBCT-phases (first phases), and for the portal venous MR- and delayed arterial DPCBCT-phases (second phases) in consensus. The percentage of enhancement was based on the percentage of the total area of enhancement seen on the axial image with the largest tumor size and was recorded in 5% increments ranging from no enhancement to 100% enhancement. Areas of tumor enhancement were considered as an indication of viable tumor, as proposed by the European Association for the Study of the Liver (EASL), and areas that were unenhanced were considered necrotic. Assessment of EASL score was limited to the two target lesions with respect to the definition of the EASL guidelines. For each nodule the percentage of tumor enhancement was assessed separately for DPCBCT and MRI according to EASL criteria. Relative change in tumor image enhancement was divided into four categories: 1) complete disappearance of tumor enhancement (100% decrease) after treatment denoted a complete response (CR); 2) $\geq$ 50% decrease in area of tumor enhancement corresponded to a partial response (PR); 3) $\geq$ 25% increase in area of tumor enhancement indicated progressive disease (PD); and 4) tumor enhancement changes that did not fit any of the previous three categories, including 0% decrease in area of tumor enhancement, were designated as stable disease (SD). An objective EASL response (OR) included CR and PR alone. For patients with two evaluated tumors, the lowest EASL response score of the two tumors was used to class EASL response per patient.

Statistical Analysis

All patient baseline characteristics data were collected and reviewed before DEB-TACE, including demographics, HCC staging, serum tests, and radiographic evaluations. One-month alpha-fetoprotein and radiographic evaluations post-DEB-TACE were also collected. The primary statistical end points of this study were area of tumor enhancement in the first and second phases at baseline and 1 month after therapy. To determine if tumor enhancement as evaluated by DPCBCT changed immediately after DEB-TACE and whether it predicted anatomical EASL tumor response at 1-month follow-up as assessed by MRI, post-DEB-TACE change in lesion enhancement for both imaging modalities were calculated as a difference between post- and pre-DEB-TACE scores according to the formula: [(% tumor enhancement$_{post}$ – % tumor enhancement$_{pre}$)/% tumor enhancement$_{pre}$] x 100, where % tumor enchancement$_{pre}$ was the baseline measurement and % tumor enhancement$_{post}$ was the post-DEB-TACE measurement. Tumors with no enhancement before and after DEB-TACE were excluded from statistical analyses to avoid misclassifying. Correlations between post-DEB-TACE changes comparing modalities, performed separately for first and second phases, were assessed using the coefficient of determination (R^2) from regressions of the change in lesion enhancement for MRI with the change in lesion enhancement for CBCT. To account for the nesting of multiple lesions within patients, ordinary least square estimation with Huber-White robust estimates of the variance were used (28). Complete, partial and objective responses were calculated using MRI data. We used a marginal generalized linear model with binomial distribution to estimate the effect of post-DEB-TACE DPCBCT lesion enhancement on the probability of each type of response

on MRI. The model was estimated using generalized estimating equations with empirical standard errors (29) and exchangeable working correlation structure to account for the within patient correlation of multiple lesions. The effect of other patient- and tumor-related characteristics was additionally explored. Lowess non-parametric smoother method was used to investigate the functional form of continuous covariates. All statistical analyses were performed using STATA software (StataCorp LP 2009; Stata Statistical Software: Release 11; College Station, TX, USA). Significance of statistical tests was assessed at the 0.05 level.

RESULTS

Patient Demographics

Twenty-seven patients with unresectable HCC (15 male; 12 female; mean age, 61.9±10.7 years; range, 30-80 years) were included in this study. All patients successfully completed both baseline pre- and post-DEB-TACE anatomical DPCBCT and MRI. Each patient underwent one selective DEB-TACE session. All procedures were performed successfully, without immediate complications. Table 1 summarizes the demographic data for this 27-patient cohort. The majority of patients had multifocal HCC with preserved underlying liver function (Child-Pugh class A disease). Most patients (55.6%, 15/27) had cirrhosis, and 44.4% were classified as Barcelona Clinic Liver Cancer (BCLC) grade C (A/B/C/D: 2/10/12/3). Overall, 47 targeted lesions were evaluated (mean, 1.7 per patient; range, 1-2): one in seven patients and two in twenty patients. The mean size of the targeted tumors at baseline was 70±48 mm (range, 11-200 mm).

One-Month MRI EASL Tumor Response Post-DEB-TACE

The 1-month follow-up anatomical contrast -enhanced T1W MR imagesdemonstrated an objective EASL response (CR or PR) in 63% and 70.4% of patients, and 74.5% and 76.6% of tumors in the first and second phases, respectively. The frequency of types of response by modality and phase, per patient and tumor are detailed in Table 2.

Intra-Procedural C-Arm Dual-Phase Cone-Beam CT Tumor Enhancement Changes and Prediction of Tumor Response After DEB-TACE

Results of paired T-test comparing change in tumor enhancement post-DEB-TACE by modality and by phase are presented in Table 3. The results are consistent with statistically significant decrease in tumor enhancement post-DEB-TACE for both modalities and both phases ($P < 0.0001$). CBCT tumor enhancement decrease post-DEB-TACE linearly correlated with MRI, estimated correlation coefficient was excellent for both first (0.79, $P < 0.0001$) (Fig. 1A) and second (0.67, $P < 0.0001$) (Fig. 1B) phases. Looking at the tumor size, the results of the T-test showed statistically significant decrease in the longest dimension of lesion after DEB-TACE ($P < 0.0001$). There was no statistically significant decrease in AFP over time ($P = 0.121$).

Table 4 presents the results of marginal generalized linear model estimating the odds or probability of objective response as a function of post-DEB-TACE CBCT tumor enhancement, pre-DEB-TACE AFP level, and pre-DEB-TACE tumor size looking at the largest diameter. In the bivariate analyses (i.e. simple logistic regression), post-DEB-TACE CBCT tumor enhancement was negatively associated with the odds of objective response in first and second phases. In the first phase, per 1 unit increment of post-DEB-TACE CBCT tumor enhancement, the odds of objective response decreased by an estimated 5% (95% Confidence Interval, CI: from 1 to 9%, $P = 0.027$). The estimate did not change after adjustment for pre-DEB-TACE AFP and tumor size. In the second phase, for 1 unit increment in post-DEB-TACE CBCT tumor enhancement, the odds of objective response decreased by an estimated 4% (95% CI: from 0 to 7%, $P = 0.034$). In multivariate analyses (i.e. the multiple logistic regression), the estimate did not change substantially. The results indicated that post-DEB-TACE CBCT tumor enhancement has independent, negative effect on the odds of objective response after accounting for pre-DEB-TACE AFP and tumor size. We

estimated that for lesions of the same size and same level of pre-DEB-TACE AFP, for each 1 unit increment in post-DEB-TACE CBCT tumor enhancement, the odds of objective response decreased by an estimated 5% (95% CI: from 1 to 9%, $P = 0.023$) and 4% (95% CI: from 1 to 7%, $P = 0.035$), in the first and second phases, respectively.

Additionally, we showed a negative, statistically significant, independent effect of pre-DEB-TACE AFP level on odds of objective response. For lesions of the same size and same post-DEB-TACE CBCT enhancement level in the second phase, the odds of objective response decreased by an estimated 0.3% (95% CI: from 0.1 to 0.4%, $P = 0.003$), in multivariate analysis. In these data, pre-DEB-TACE tumor size did not affect the odds of objective response after accounting for the pre-DEB-TACE AFP level and post-DEB-TACE CBCT tumor enhancement ($P = 0.810$ and 0.359 for first and second phase, respectively). Due to the small numbers of patients achieving SD or PD, we do not present the effect of post-DEB-TACE CBCT tumor enhancement on 1-month EASL MR response for these categories. Figures 2 and 3 are composed of representative DPCBCT images from single patients showing HCC enhancement changes during DEB-TACE and corresponding EASL tumor response on MRI 1 month later.

DISCUSSION

This study investigated the usefulness of intra-procedural post-DEB-TACE dual-phase CBCT imaging for the prediction of 1-month objective EASL HCC tumor response . Our results show good sensitivity to the ability of the intra-procedural DPCBCT imaging study to monitor and quantify HCC enhancement changes during DEB-TACE. There was overall excellent accuracy of the intra-procedural immediate post-therapy DPCBCT imaging scan in predicting future response to therapy.

Early determination of therapeutic response may be helpful to guide patient management decisions after chemoembolization, especially regarding the need for repeat treatment. Recently, vascular and cellular biomarkers including contrast enhancement and ADC values from diffusion-weighted MR imaging (DWI) have been shown to change within hours to days after therapy, which is earlier than changes seen by conventional HCC anatomical size assessment (30–35). Nevertheless, the optimum time after TACE for patients to undergo imaging is unknown. Some authors have suggested that contrast-enhanced ultrasonography (CEUS) performed ≥ 2 days after TACE could be predictive of tumor outcome (36), whereas others showed that CEUS results 1 week after TACE were consistent with those of dynamic CT performed 2 months after intervention (37). Several previous clinical studies have shown the ability of DWI to map water distribution within HCC tumors and to quantify tumor necrosis after transcatheter liver-directed therapy (34,38,39). Chung et al. (18) have even recently reported for the first time that intra-procedural ADC changes assessed in a hybrid MR/IR suite can predict 1-month anatomical HCC response and provide valuable feedback at the time of TACE. They

found that patients whose intra-procedural ADC values increase or decrease by > 15% are more likely to have a favorable anatomical tumor response 1 month later. None of the aforementioned studies, however, were able to address the question of whether tumor enhancement changes at the time of chemoembolization could be used to predict future EASL response. Now, even if some authors suggest that very early assessment may not be appropriate in the case of TACE with LC Beads because the degree of necrosis could be underestimated (5,40), we think the emphasis should be on monitoring immediate changes in tumor enhancement since the ADC value changes and the availability of hybrid MR/IR suites may be limited. We were able to address this gap in knowledge through the use of an integrated CBCT/IR suite. Such a suite allowed us to image patients with dual-phase CBCT imaging immediately before and after DEB-TACE, allowing for tumor imaging at both early and delayed arterial phases using only one contrast injection, and without the need for multiple patient transfers as reported between the DSA unit and the adjacent MR unit during the TACE procedure with hybrid MR/IR suites (18). Using this setup, we were able to show that DPCBCT imaging could be used intra-procedurally to predict a future anatomical objective response 1 month after DEB-TACE. A positive result would likely suggest adequate HCC treatment; however, a negative result would not be useful feedback and could not be interpreted as insufficient treatment.

Contrast enhancement is a reflection of cellular viability (30–32): areas of tumor enhancement are considered viable, whereas unenhanced regions reflect tissue necrosis, as suggested by the European Association for the Study of Liver Disease. To accurately assess tumor enhancement, we used C-arm CT that has emerged as a worldwide popular generation of imaging technology available in the angiography suite, allowing for the acquisition of a three-dimensional dataset generated from one

rotational run with the use of cone-beam CT principles (CBCT) (19-23). Compared with conventional DSA, CBCT imaging can provide additional useful information for patients undergoing TACE (19–23). Similarly, early and on-going clinical experience has demonstrated that CBCT using dual-phase imaging can provide better information than DSA for TACE and, occasionally, conventional CT or MRI in terms of detectability of liver tumors (26,27). Furthermore, dual-phase CBCT has a benefit over CE-MRI in that CBCT imaging can be done during the TACE procedure with minimal additional effort than x-ray DSA and fluoroscopy. This can provide live-image feedback not only on the DEB-TACE delivery catheter positioning and drug delivery amount, but also on embolization success, as shown in our study.

This study had several limitations. First, the sample was small, with possible selection bias since we included only 27 of 47 patients whose care was discussed by our liver tumor board during the enrollment period. Second, histopathologic data were not obtained for any of the patients in the study. Therefore, tumor cell death was measured only with MRI. Previous reports (30–32), however, have shown good correlation between the histopathologic percentage of necrosis and the tumor enhancement obtained with MRI. Third, monitoring therapeutic effect with CBCT would increase radiation and iodine contrast load for the patient, in comparison with MRI. However, the x-ray effective dose from CBCT imaging is significantly less than a typical abdomen scan using diagnostic multi-detector CT, even when four CBCT scans (2 dual-phase acquisitions: one pre- and one post-embolization) are performed (26,41). Furthermore, the use of dual-phase technology reduces the use of iodinated contrast medium by 50% for the CBCT component of the interventional procedure while allowing for visualization of changes in temporal enhancement before and after drug-eluting beads treatment. Finally, we do not have long-term evaluation of patient

outcomes and cannot yet state that patients with tumor response have different, presumably better, outcomes than patients who do not have tumor response. The results of this study need to be validated by future studies with larger cohorts and longer follow-up time to determine if intra-procedural DPCBCT tumor enhancement changes reliably predict patient prognosis or affect outcome.

In conclusion, our study showed that intra-procedural DPCBCT tumor enhancement changes could serve as a useful prognostic indicator of HCC response to DEB-TACE. These preliminary results are encouraging because early knowledge of HCC response after initial therapy is essential to revise prognosis and guide future therapy. Use of DPCBCT at the time of DEB-TACE could improve treatment planning.

REFERENCES

1. El-Serag HB, Rudolph KL. Hepatocellular carcinoma: epidemiology and molecular carcinogenesis. Gastroenterology 2007;132:2557–2576.
2. Bosch FX, Ribes J, Díaz M, Cléries R. Primary liver cancer: worldwide incidence and trends. Gastroenterology 2004;127:S5–S16.
3. Llovet JM, Real MI, Montaña X, et al. Barcelona Liver Cancer Group. Arterial embolisation or chemoembolisation versus symptomatic treatment in patients with unresectable hepatocellular carcinoma: a randomised controlled trial. Lancet 2002;359:1734 –1739.
4. Lo CM, Ngan H, Tso WK, et al. Randomized controlled trial of transarterial lipiodol chemoembolization for unresectable hepatocellular carcinoma. Hepatology 2002;35:1164 –1171.
5. Hong K, Khwaja A, Liapi E, Torbenson MS, Georgiades CS, Geschwind JF. New intra-arterial drug delivery system for the treatment of liver cancer: preclinical assessment in a rabbit model of liver cancer. Clin Cancer Res 2006;12:2563–2567.
6. Lewis AL, Gonzalez MV, Leppard SW, et al. Doxorubicin eluting beads–1: effects of drug loading on bead characteristics and drug distribution. J Mater Sci Mater Med 2007;18:1691–1699.
7. Varela M, Real MI, Burrel M, et al. Chemoembolization of hepatocellular carcinoma with drug eluting beads: efficacy and doxorubicin pharmacokinetics. J Hepatol 2007;46:474–481.
8. Poon RT, Tso WK, Pang RW, et al. A phase I/II trial of chemoembolization for hepatocellular carcinoma using a novel intra-arterial drug-eluting bead.

Clin Gastroenterol Hepatol 2007;5:1100–1108.

9. Malagari K, Alexopoulou E, Chatzimichail K, et al. Transcatheter chemoembolization in the treatment of HCC in patients not eligible for curative treatments: midterm results of doxorubicin-loaded DC bead. Abdom Imaging 2008;33:512–519.
10. Reyes DK, Vossen JA, Kamel IR, et al. Single-center phase II trial of transarterial chemoembolization with drug-eluting beads for patients with unresectable hepatocellular carcinoma: initial experience in the United States. Cancer J 2009;15:526–532.
11. Lammer J, Malagari K, Vogl T, et al; PRECISION V Investigators. Prospective randomized study of doxorubicin-eluting-bead embolization in the treatment of hepatocellular carcinoma: results of the PRECISION V study. Cardiovasc Intervent Radiol 2010;33:41–52.
12. Therasse P, Arbuck SG, Eisenhauer EA, et al. New guidelines to evaluate the response to treatment in solid tumors. European Organization for Research and Treatment of Cancer, National Cancer Institute of the United States, National Cancer Institute of Canada. J Natl Cancer Inst 2000;92:205–216.
13. Tsuchida Y, Therasse P. Response evaluation criteria in solid tumors (RECIST): new guidelines. Med Pediatr Oncol 2001;37:1–3.
14. Lencioni R, Llovet JM. Modified RECIST (mRECIST) assessment for hepatocellular carcinoma. Semin Liver Dis 2010;30:52–60.
15. Bruix J, Sherman M, Llovet JM, et al. Clinical management of hepatocellular carcinoma. Conclusions of the Barcelona-2000 EASL conference. European Association for the Study of the Liver. J Hepatol 2001;35:421–430.
16. Lim HK, Han JK. Hepatocellular carcinoma: evaluation of therapeutic

response to interventional procedures. Abdom Imaging 2002;27:168–179.

17. Bruix J, Sherman M. Management of hepatocellular carcinoma. Hepatology 2005;42:1208–1236.
18. Chung JC, Naik NK, Lewandowski RJ, et al. Diffusion-weighted magnetic resonance imaging to predict response of hepatocellular carcinoma to chemoembolization. World J Gastroenterol 2010;16:3161–3167.
19. Kakeda S, Korogi Y, Ohnari N, et al. Usefulness of cone-beam CT with flat panel detectors in conjunction with catheter angiography for transcatheter arterial embolization. J Vasc Interv Radiol 2007;18:1508–1516.
20. Wallace MJ, Kuo MD, Glaiberman C, Binkert CA, Orth RC, Soulez G. Three-dimensional C-arm cone-beam CT: applications in the interventional suite. J Vasc Interv Radiol 2008;19:799–813.
21. Orth RC, Wallace MJ, Kuo MD. C-arm cone-beam CT: general principles and technical considerations for use in interventional radiology. J Vasc Interv Radiol 2008;19:814–821.
22. Miyayama S, Yamashiro M, Okuda M, et al. Usefulness of cone-beam computed tomography during ultraselective transcatheter arterial chemoembolization for small hepatocellular carcinomas that cannot be demonstrated on angiography. Cardiovasc Intervent Radiol 2009;32:255–264.
23. Miyayama S, Matsui O, Yamashiro M, et al. Detection of hepatocellular carcinoma by CT during arterial portography using a cone-beam CT technology: comparison with conventional CTAP. Abdom Imaging 2009;34:502–506.
24. Geschwind JF, Ramsey DE, Cleffken B, et al. Transcatheter arterial chemoembolization of liver tumors: effects of embolization protocol on

injectable volume of chemotherapy and subsequent arterial patency. Cardiovasc Intervent Radiol 2003;26:111–117.

25. Feldkamp LA, Davis LC, Kress JW. Practical cone-beam algorithm. J Opt Soc Am 1984;A1:612–619.
26. Lin M, Loffroy R, Noordhoek N, et al. Evaluating tumors in transcatheter arterial chemoembolization (TACE) using dual-phase cone-beam CT. Minim Invasive Ther Allied Technol 2010;[Epub ahead of print].
27. Miyayama S, Yamashiro M, Okuda M, et al. Detection of corona enhancement of hypervascular hepatocellular carcinoma by C-arm dual-phase cone-beam CT during hepatic arteriography. Cardiovasc Intervent Radiol 2010;[Epub ahead of print].
28. Williams RL. A note on robust variance estimation for cluster-correlated data. Biometrics 2000;56:645–646.
29. Diggle PJ, Liang KY, Zeger SL. Analysis of Longitudinal Data. Oxford, Pa: Oxford University Press, 1994;146–162.
30. Murakami T, Nakamura H, Hori S, et al. Detection of viable tumor cells in hepatocellular carcinoma following transcatheter arterial chemoembolization with iodized oil: pathologic correlation with dynamic turbo-FLASH MR imaging with Gd-DTPA. Acta Radiol 1993;34:399–403.
31. Castrucci M, Sironi S, De Cobelli F, Salvioni M, Del Maschio A. Plain and gadolinium-DTPA-enhanced MR imaging of hepatocellular carcinoma treated with transarterial chemoembolization. Abdom Imaging 1996;21:488–494.
32. Bartolozzi C, Lencioni R, Caramella D, Mazzeo S, Ciancia EM. Treatment of hepatocellular carcinoma with percutaneous ethanol injection: evaluation with contrast-enhanced MR imaging. AJR Am J Roentgenol 1994;162:827–831.

33. Ross BD, Moffat BA, Lawrence TS, et al. Evaluation of cancer therapy using diffusion magnetic resonance imaging. Mol Cancer Ther 2003;2:581–587.
34. Kamel IR, Liapi E, Reyes DK, Zahurak M, Bluemke DA, Geschwind JF. Unresectable hepatocellular carcinoma: serial early vascular and cellular changes after transarterial chemoembolization as detected with MR imaging. Radiology 2009;250:466–473.
35. Kalb B, Chamsuddin A, Nazzal L, Sharma P, Martin DR. Chemoembolization follow-up of hepatocellular carcinoma with MR imaging: usefulness of evaluating enhancement features on one-month posttherapy MR imaging for predicting residual disease. J Vasc Interv Radiol 2010;21:1396–1404.
36. Kono Y, Lucidarme O, Choi SH, et al. Contrast-enhanced ultrasound as a predictor of treatment efficacy within 2 weeks after transarterial chemoembolization of hepatocellular carcinoma. J Vasc Interv Radiol 2007;18:57–65.
37. Xia Y, Kudo M, Minami Y, et al. Response evaluation of transcatheter arterial chemoembolization in hepatocellular carcinomas: the usefulness of sonazoid-enhanced harmonic sonography. Oncology 2008;75:99–105.
38. Kamel IR, Bluemke DA, Eng J, et al. The role of functional MR imaging in the assessment of tumor response after chemoembolization in patients with hepatocellular carcinoma. J Vasc Interv Radiol 2006;17:505–512.
39. Chen CY, Li CW, Kuo YT, et al. Early response of hepatocellular carcinoma to transcatheter arterial chemoembolization: choline levels and MR diffusion constants–initial experience. Radiology 2006;239:448–456.
40. Moschouris H, Malagari K, Papadaki MG, Kornezos I, Matsaidonis D. Contrast-enhanced ultrasonography of hepatocellular carcinoma after

chemoembolisation using drug-eluting beads: a pilot study focused on sustained tumor necrosis. Cardiovasc Intervent Radiol 2010;33:1022–1027.

41. Racadio J, Yoshizumi T, Toncheva G, Stueve D, Anderson-Evans C, Frush D. Radiation dosimetry evaluation of C-arm cone beam CT for pediatric interventional radiology procedures: a comparison with MDCT. In: RSNA. Chicago, IL, USA, 2008.

TABLES

TABLE 1.

Baseline characteristics of patients with hepatocellular carcinoma prior to treatment.

Baseline Characteristics	Value (*n* or mean ± SD)
Demographics	
No. patients/No. tumors evaluated	27/47
Age (Year)	61.9 ± 10.7
Sex (Male/Female)	15/12
Race (White/African-American/Hispanic/Other)	12/7/2/6
Etiology (Alcohol/HCV/HBV/NASH/Cryptogenic)	2/12/2/2/9
ECOG performance status (0/1/2/3/4)	15/10/2/0/0
Cirrhosis (Present/Absent)	15/12
Type (Unifocal/Multifocal/Diffuse)	6/12/9
Portal vein thrombosis (Yes/No)	8/19
Tumor size* (mm)	70 ± 48
HCC staging	
Child-Pugh class (A/B/C)	19/6/2
BCLC stage (A/B/C/D)	2/10/12/3
Okuda stage (I/II/III)	11/15/1
CLIP score (1/2/3/4/5)	8/11/5/2/1
Serum tests	
Basal AFP (ng/mL)	38 209 ± 176 640
<10	9
10-200	8
>200	10
Albumin (g/dL)	3.6 ± 0.8
Total bilirubin (mg/dL)	1.8 ± 3.4
AST (U/L)	129.6 ± 78.6
ALT (U/L)	103.8 ± 83.5
Alkaline phosphatase (U/L)	244.8 ± 260.7
INR	1.2 ± 0.7

Note.–HCV, Hepatitis C Virus; HBV, Hepatitis B Virus; NASH, Non-Alcoholic Steato-Hepatitis; ECOG, Eastern Cooperative Oncology Group; HCC, Hepatocellular Carcinoma; BCLC, Barcelona Clinic Liver Cancer; CLIP, Cancer of the Liver Italian Program; AFP, Alpha-Feto-Protein; AST, Aspartate Aminotransferase; ALT, Alanine Aminotransferase; INR, International Normalized Ratio. * One-dimensional measure of the longest dimension as measured by MRI.

TABLE 2.

Frequency of different types of EASL response by modality and by phase, per patient and per tumor.

Response	MRI				CBCT			
	First phase		Second phase		First phase		Second phase	
	P	T	P	T	P	T	P	T
CR	1 (3.7)	3 (6.4)	4 (14.8)	13 (27.7)	3 (11.1)	7 (14.9)	3 (11.1)	10 (21.3)
PR	16 (59.3)	32 (68.1)	15 (55.6)	23 (48.9)	18 (66.7)	30 (63.8)	11 (40.7)	17 (36.2)
SD	9 (33.3)	11 (23.4)	6 (22 .2)	8 (17)	6 (22.2)	10 (21.3)	10 (37)	17 (36.2)
PD	1 (3.7)	1 (2.1)	2 (7.4)	3 (6.4)	0 (0)	0 (0)	3 (11.1)	3 (6.4)
OR	17 (63)	35 (74.5)	19 (70.4)	36 (76.6)	21 (78.8)	37 (78.7)	14 (51.8)	27 (57.5)

Note.–Data are *n* (%). EASL, European Association for the Study of Liver Disease; MRI, Magnetic Resonance Imaging; CBCT, Cone-Beam Computed Tomography; P, Patients (*n* = 27); T, Tumors (*n* = 47); CR, Complete Response; PR, Partial Response; SD, Stable Disease; PD, Progressive Disease; OR, Objective Response (CR + PR).

TABLE 3.

Changes in tumor size, tumor enhancement by modality and by phase, and AFP value after DEB-TACE (*n* = 27).

Features	Before DEB-TACE	After DEB-TACE	Change (%)	*P* Value
Tumor size* (mm)	70 ± 48	66 ± 46	6	<0.0001
Tumor enhancement (%)				
MRI				
First phase	56 ± 30	22 ± 22	61	<0.0001
Second phase	26 ± 25	11 ± 17	58	<0.0001
CBCT				
First phase	54±27	20 ± 19	63	<0.0001
Second phase	30 ± 27	15 ± 23	50	<0.0001
AFP (ng/mL)	38209 ± 176640	11214 ± 43947	71	0.121

Note.–Data are means ± SD or %. $P < .05$ was considered statistically significant. DEB-TACE, Drug-Eluting Bead Transcatheter Arterial Chemoembolization; MRI, Magnetic Resonance Imaging; CBCT, Cone-Beam Computed Tomography; AFP, Alpha-Feto-Protein. * One-dimensional measure of the longest dimension as measured by MRI.

TABLE 4.

Results of GEE logistic regression models predicting the probability of 1-month MRI objective (complete or partial) EASL response as a function of covariates.

Variables	Simple Logistic Regression			Multiple Logistic Regression		
	OR	**95%CI**	***P* Value**	**OR**	**95%CI**	***P* Value**
First Phase						
Post-DEB-TACE CBCT TE*	0.950	0.910-0.990	0.027	0.950	0.910-0.990	0.023
Pre-DEB-TACE AFP†	1.010	0.900-1.140	0.839	1.004	0.997-1.011	0.264
Pre-DEB-TACE size‡ (mm)	0.999	0.984-1.015	0.946	0.998	0.986-1.010	0.810
Second Phase						
Post-DEB-TACE CBCT TE*	0.960	0.930-1.000	0.034	0.960	0.930-0.990	0.035
Pre-DEB-TACE AFP†	0.998	0.997-0.999	0.005	0.997	0.996-0.999	0.003
Pre-DEB-TACE size‡ (mm)	0.990	0.980-1.000	0.075	0.990	0.980-1.010	0.359

Note.–$P < 0.05$ was considered statistically significant. EASL, European Association for the Study of Liver Disease; MRI, Magnetic Resonance Imaging; OR, Odds Ratio; CI, Confidence Interval; DEB-TACE, Drug-Eluting Bead Transcatheter Arterial Chemoembolization; CBCT, Cone-Beam Computed Tomography; TE, Tumor Enhancement; AFP, Alpha-Feto-Protein. * For every increment; † per 1000 units; ‡ One-dimensional measure of the longest dimension as measured by MRI.

FIGURE CAPTIONS

Figure 1: *A–B,* Scatter-plot graphs show correlation of tumor enhancement changes in first (early arterial or arterial) and second (delayed arterial or portal venous) phase post-DEB-TACE measured with CBCT and MRI. CBCT tumor enhancement decrease post-DEB-TACE linearly correlated with MRI, estimated correlation coefficient was excellent for both first (0.79, $P < 0.0001$) and second (0.67, $P < 0.0001$) phases.

Figure 2: *A–D,* Representative T1-weighted enhanced arterial or first and portal venous or second phase MR images (left), and enhanced early or first and delayed or second arterial phase CBCT images (right) from a 73-year-old man with right-lobe cryptogenic HCC. MR images were acquired approximately 1 month before and after DEB-TACE therapy, whereas dual-phase CBCT images were acquired prior to and immediately following DEB-TACE. *A,* First phase baseline pre-DEB-TACE images. Left: A 75-mm mass in right lobe shows 65% enhancement. Right: Mass shows almost similar enhancement (75%). *B,* Second phase baseline pre-DEB-TACE images. Left: Mass shows 60% enhancement. Right: Mass shows almost similar enhancement (70%). *C,* First phase post-DEB-TACE images. Left: Mass shows almost no enhancement (5%), tumor changed to 69-mm in size. Right: Intra-procedural mass enhancement changed by 86.7%, which predicted an objective EASL response at 1 month. *D,* Second phase post-DEB-TACE images. Left: Mass shows no enhancement (0%). Right: Intra-procedural mass enhancement changed by 92.9%, which predicted an objective EASL response at 1 month.

Figure 3: *A–D,* Representative enhanced first and second phase MR (left) and CBCT (right) images from a 58-year-old man with right-lobe HCC secondary to hepatitis Cvirus . MR images were acquired approximately 1 month before and after DEB-TACE therapy, while dual-phase CBCT images were acquired prior to and immediately following DEB-TACE. *A,* First phase baseline pre-DEB-TACE images. Left: A 32-mm mass in right lobe shows 75% enhancement (arrows). Right: Mass shows almost similar enhancement (80%) (arrows). *B,* Second phase baseline pre-DEB-TACE images. Left: Mass shows partial wash-out (50% enhancement) (arrows). Right: Mass shows almost same enhancement reduction (65%) (arrows). *C,* First phase post-DEB-TACE images. Left: Mass shows almost no enhancement (5%), tumor remains unchanged in size (31-mm) (arrows). Right: Intra-procedural mass enhancement (arrows)changed by 100%, which predicted an objective EASL response at 1 month. *D,* Second phase post-DEB-TACE images. Left: Mass shows almost no enhancement (5%) (arrows). Right: Intra-procedural mass enhancement (arrows) changed by 92.3%, which predicted an objective EASL response at 1 month.

FIGURES

Figure 1

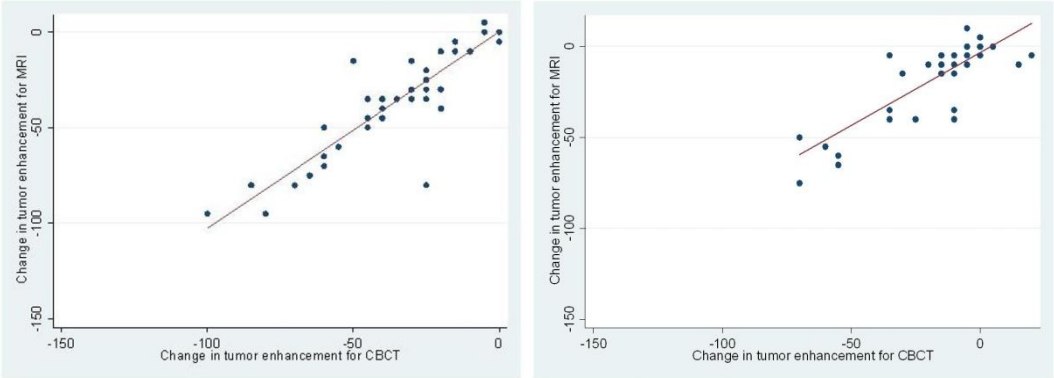

Figure 2

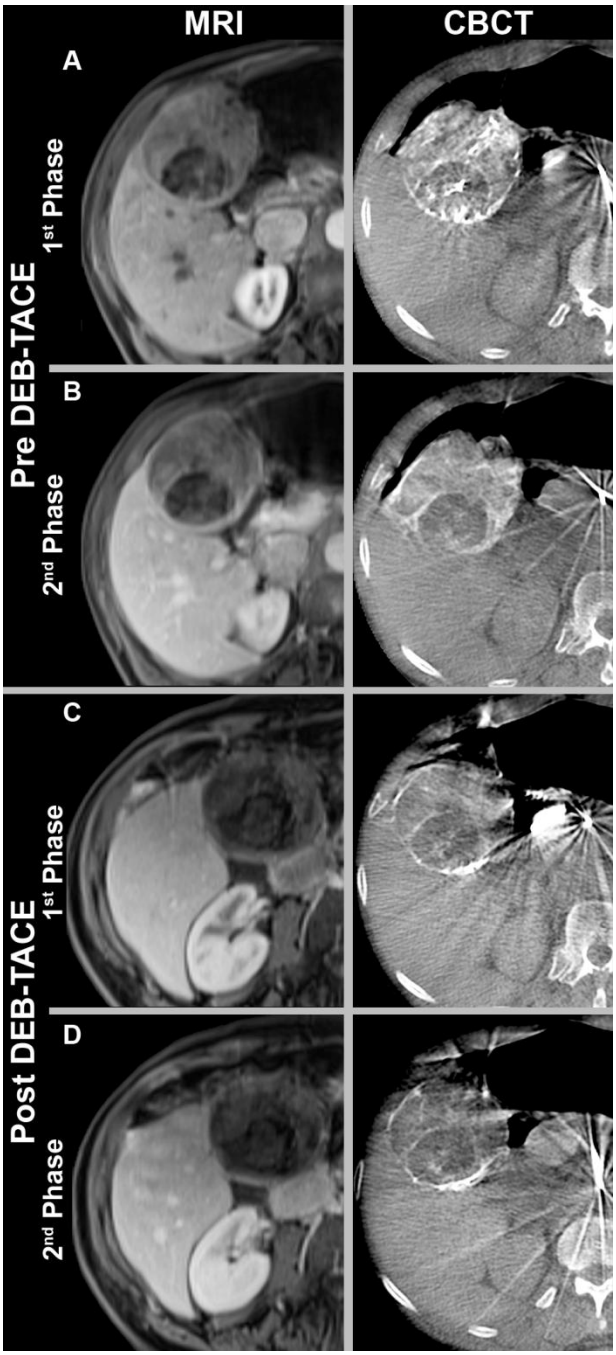
MRI
CBCT
A
1st Phase
Pre DEB-TACE
B
2nd Phase
C
1st Phase
Post DEB-TACE
D
2nd Phase

Figure 3

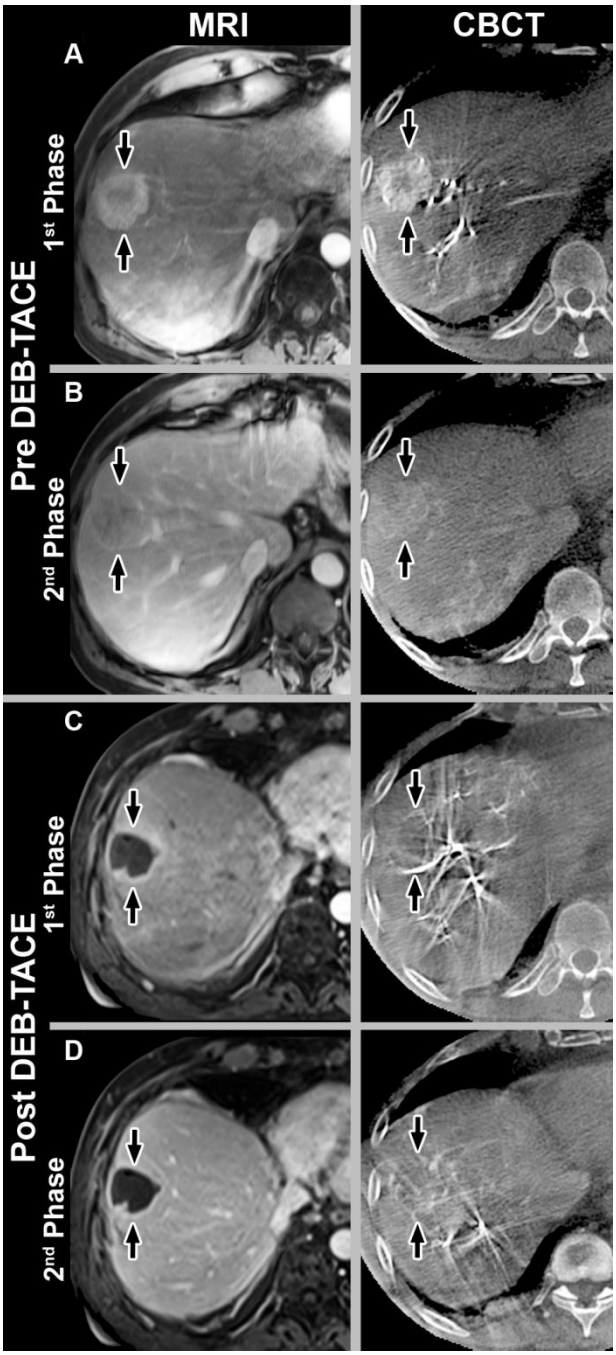
MRI
CBCT
A
1st Phase
Pre DEB-TACE
B
2nd Phase
C
1st Phase
Post DEB-TACE
D
2nd Phase